JCB Article

Microdomains of the C-type lectin DC-SIGN are portals for virus entry into dendritic cells

Alessandra Cambi,[1] Frank de Lange,[1] Noortje M. van Maarseveen,[4] Monique Nijhuis,[4] Ben Joosten,[1] Erik M.H.P. van Dijk,[5] Bärbel I. de Bakker,[5] Jack A.M. Fransen,[2] Petra H.M. Bovee-Geurts,[3] Frank N. van Leeuwen,[1] Niek F. Van Hulst,[5] and Carl G. Figdor[1]

[1]Department of Tumor Immunology, [2]Department of Cell Biology, and [3]Department of Medical Biochemistry, Nijmegen Center for Molecular Life Sciences, University Medical Center Nijmegen, 6500 HB Nijmegen, Netherlands
[4]Department of Virology, University Medical Center Utrecht, 3508 GA Utrecht, Netherlands
[5]Applied Optics Group, Department of Science and Technology, Molecular Engineering Sensors and Actuators Research Institute for Nanotechnology, University of Twente, 7500 AE Enschede, Netherlands

The C-type lectin dendritic cell (DC)–specific intercellular adhesion molecule grabbing non-integrin (DC-SIGN; CD209) facilitates binding and internalization of several viruses, including HIV-1, on DCs, but the underlying mechanism for being such an efficient phagocytic pathogen-recognition receptor is poorly understood. By high resolution electron microscopy, we demonstrate a direct relation between DC-SIGN function as viral receptor and its microlocalization on the plasma membrane. During development of human monocyte-derived DCs, DC-SIGN becomes organized in well-defined microdomains, with an average diameter of 200 nm. Biochemical experiments and confocal microscopy indicate that DC-SIGN microdomains reside within lipid rafts. Finally, we show that the organization of DC-SIGN in microdomains on the plasma membrane is important for binding and internalization of virus particles, suggesting that these multimolecular assemblies of DC-SIGN act as a docking site for pathogens like HIV-1 to invade the host.

Introduction

In the past two years, several new genes have been identified encoding leukocyte-specific carbohydrate binding proteins that belong to the lectin-like receptors family (Kogelberg and Feizi, 2001; Figdor et al., 2002). Many of these lectins are members of the calcium-dependent C-type lectin family and recognize their ligands through the structurally related Ca^{2+}-dependent carbohydrate-recognition domains (C-type CRDs; Drickamer, 1999). Many C-type lectins act as cell adhesion receptors (Vestweber and Blanks, 1999), whereas others are specialized in antigen recognition (Stahl and Ezekowitz, 1998; Mahnke et al., 2000).

Dendritic cells (DCs) constitute a specific group of professional antigen presenting leukocytes, constantly patrolling the body for foreign intruders (Steinman 1991; Banchereau and Steinman, 1998). DCs are equipped with a variety of dynamically regulated pathogen-recognition receptors. Although some of them are members of the toll-like receptor (TLR) family, signaling molecules specialized in sensing pathogens (Akira, 2003), others belong to the C-type lectin family and mediate pathogen binding and uptake (Stahl and Ezekowitz, 1998; Mahnke et al., 2000).

DC-specific intercellular adhesion molecule (ICAM) grabbing non-integrin (DC-SIGN; CD209) is a C-type lectin specifically expressed by DCs and has a dual function. As an adhesion receptor, DC-SIGN supports initial DC–T cell interaction by binding to ICAM-3 (Geijtenbeek et al., 2000a), and mediates tethering and rolling of DCs on the endothelium by interacting with ICAM-2 (Geijtenbeek et al., 2000c). As a pathogen-recognition receptor, DC-SIGN binds HIV gp120 thus facilitating the transport of HIV from mucosal sites to draining lymph nodes where infection of T lymphocytes occurs (Geijtenbeek et al., 2000b). Recently, DC-SIGN was also shown to bind other viruses like CMV (Halary et al., 2002), Ebola (Alvarez et al., 2002), Dengue (Tassaneetrithep et al., 2003), and hepatitis C (Lozach et al., 2003; Pöhlmann et al., 2003), as well as microorganisms

The online version of this article contains supplemental material.

Address correspondence to Carl G. Figdor, Dept. of Tumor Immunology, Nijmegen Center for Molecular Life Sciences, University Medical Center Nijmegen, P.O. Box 9101, 6500 HB Nijmegen, Netherlands. Tel.: 31-24-361-7600. Fax: 31-24-354-0339.
email: c.figdor@ncmls.kun.nl

Key words: pathogen recognition receptor; lectin; electron microscopy; multiprotein assembly; lipid rafts

The Journal of Cell Biology, Volume 164, Number 1, January 5, 2004 145–155
http://www.jcb.org/cgi/doi/10.1083/jcb.200306112

Supplemental Material can be found at:
http://www.jcb.org/cgi/content/full/jcb.200306112/DC1

such as *Leishmania* (Colmenares et al., 2002), *Candida albicans* (Cambi et al., 2003), *Mycobacterium* (Geijtenbeek et al., 2003; Maeda et al., 2003; Tailleux et al., 2003), and *Schistosoma* (van Die et al., 2003).

Recent works have demonstrated that some microbial pathogens exploit cholesterol-enriched lipid microdomains as essential docking sites to enter host cells (Gatfield and Pieters, 2000; Rosenberger et al., 2000; Lafont et al., 2002). These microdomains, also known as lipid rafts, are localized regions with elevated cholesterol and glycosphingolipid content that can be found on the plasma- and endosomal-membrane of eukaryotic cells (London and Brown, 2000; Simons and Toomre, 2000; Simons and Ehehalt, 2002). Some viruses, such as HIV-1, appear to target lipid raft microdomains during viral entry into cells, as well as during viral assembly before budding from cells (Dimitrov, 1997; Mañes et al., 2000). Other works suggest that cholesterol-dependent membrane properties, rather than lipid rafts per se, are responsible to promote efficient HIV-1 infection in T cells (Percherancier et al., 2003).

DC-SIGN, like other C-type lectins, recognizes pathogens by binding to carbohydrate moieties in a Ca^{2+}-dependent manner, through a conserved CRD (Drickamer, 1999). This CRD has a high specificity for complex mannose residues and is located at the distal end of the extracellular domain (ECD), which consists of several amino acid repeats (Soilleux et al., 2000). Recently, purified truncated forms of DC-SIGN containing either the complete ECD or only the CRD were used to analyze the quaternary structure as well as the affinity of DC-SIGN for its ligands. Biochemical experiments indicated that in vitro ECDs aggregate to form tetramers, thus enhancing DC-SIGN capacity to bind multivalent ligands, such as pathogen sugar arrays (Mitchell et al., 2001). Surface plasmon resonance experiments showed that whereas the ECD readily binds hepatitis C virus glycoprotein E2, distant monomeric CRDs do not, unless closely seeded (Lozach et al., 2003).

These findings suggest that the organization of DC-SIGN molecules on the plasma membrane may be critical for pathogen binding. This prompted us to investigate the cell surface distribution pattern of DC-SIGN and its possible association with lipid rafts. Using transmission EM (TEM) on whole-mount samples of transfected cells and monocyte-derived DCs, we have mapped the microlocalization of DC-SIGN at high resolution. Subsequently, spatial-point pattern analysis showed that DC-SIGN is organized in well-defined microdomains. Moreover, biochemical experiments and confocal microscopy analysis demonstrated that DC-SIGN colocalizes with lipid rafts. Finally, we show that these microdomains of DC-SIGN act as a docking site for HIV-1 particles, facilitating entry of the virus into DCs.

Results

DC-SIGN is organized in microdomains on the cell surface

To study the correlation between functional state and cell surface organization of DC-SIGN, we used K562 transfectants stably expressing DC-SIGN. K-DC-SIGN expressed high levels of DC-SIGN (Fig. 1 A) and bound strongly to

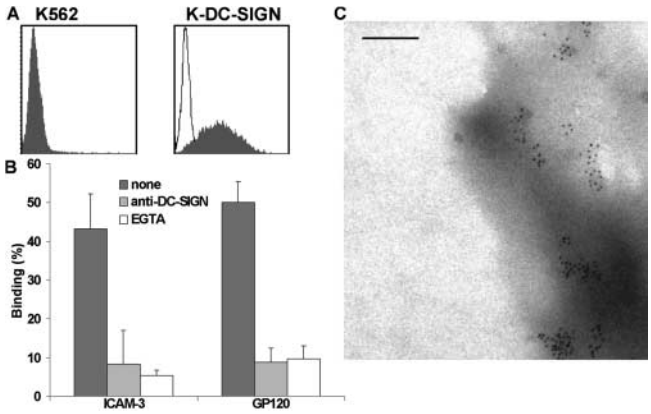

Figure 1. **DC-SIGN is organized in microdomains on the cell surface of K-DC-SIGN.** (A) The expression levels of DC-SIGN on untransfected K562 and on K-DC-SIGN were assessed by FACS® analysis. The open histogram represents the isotype control, and shaded histogram indicates the specific staining with anti–DC-SIGN (AZN-D1). (B) DC-SIGN expressed by K562 transfectants strongly binds to ICAM-3 and gp120. The adhesion was determined using 1-μm ligand-coated fluorescent beads. Specificity was determined by measuring binding in presence of AZN-D1. No blocking was observed in presence of isotype control (not depicted). Blocking exerted by EGTA indicates that DC-SIGN binds to the ligands in a Ca^{2+}-dependent manner. The average of five independent experiments is shown ($P < 0.001$). (C) K-DC-SIGN cells were specifically labeled with 10-nm gold particles, as described in Materials and methods. Cells were allowed to adhere onto poly-L-lysine–coated formvar film and photographed in an electron microscope. Gold particles were detected on the periphery on the thinner less electron dense parts of cells, where good contrast could be achieved. One representative picture is shown. Bar, 200 nm.

1-μm fluorescent beads coated with ICAM-3 or GP120 (Fig. 1 B). The binding of K-DC-SIGN to these ligands was specific, as shown by the inhibition exerted by anti–DC-SIGN mAbs. Moreover, the lack of adhesion in presence of EGTA confirmed that DC-SIGN bound to these ligands in a Ca^{2+}-dependent manner, typical of C-type lectin-like receptors.

To determine the organization of DC-SIGN on the cell membrane at high resolution, TEM was used on whole-mount samples of K-DC-SIGN, after specific labeling with anti–DC-SIGN mAb and 10-nm gold particles. It should be noted that the specimens were not sectioned thus making the whole cell surface available for gold labeling and subsequent TEM analysis. This method has been successfully applied to detect spatial distribution of other membrane proteins such as the potassium channels Kv1.3 (Panyi et al., 2003) and the IL-2 receptor α-subunit (Vereb et al., 2000). As shown in Fig. 1 C, DC-SIGN showed a clear distribution in well-defined microdomains on K-DC-SIGN plasma membrane. These microdomains had an average diameter of 200 nm and appeared to be randomly localized on the cell surface. To exclude that the gold labeling pattern observed could be due to internalized DC-SIGN molecules; also, sections of these cell samples were analyzed by TEM. The results demonstrated that the gold particles were exclusively detected on the outside of the cell membrane (unpublished data), confirming the presence of DC-SIGN in microdomains on the cell surface. To show that the clustering of DC-SIGN is not an artifact due to the procedure, we also analyzed by TEM other trans-

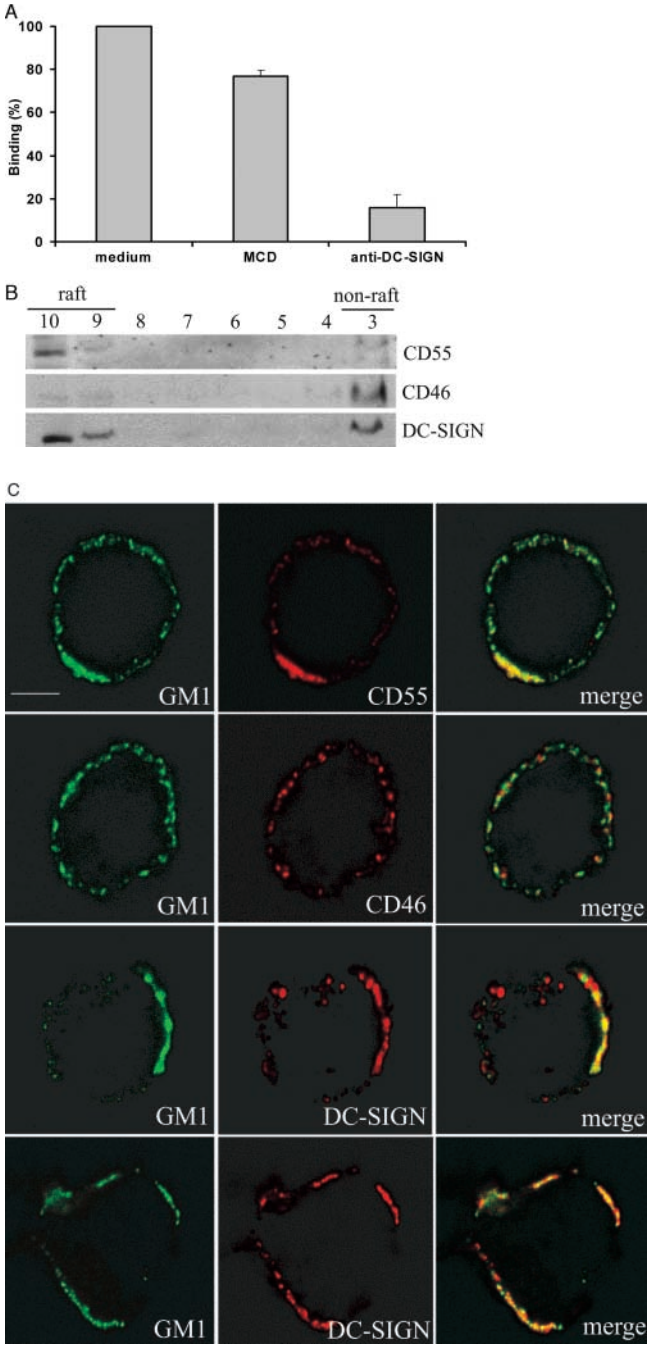

Figure 2. **DC-SIGN colocalizes with lipid rafts on K-DC-SIGN.** (A) To investigate the effect of cholesterol depletion on DC-SIGN–mediated adhesion, K-DC-SIGN cells were incubated in serum-free medium with or without 20 mM MCD for 30 min at 37°C. Subsequently, gp120-coated fluorescent beads (1-μm diam) were added and the mixture was incubated for an additional 30 min at 37°C. Binding was measured by flow cytometry. After MCD treatment, cell viability was assessed by trypan blue staining. The values represent the mean of three independent experiments ±SD. (B) K-DC-SIGN were solubilized with 1% Triton X-100, subjected to sucrose gradient centrifugation and analyzed by Western blotting for the indicated molecules. The numbers indicate the gradient fractions. Fractions 9 and 10 are low density fractions containing DRM and are referred to as raft fractions. (C) Confocal microscopy analysis of copatching of DC-SIGN and GM1. K-DC-SIGN cells were stained at 4°C with 10 μg/ml anti–DC-SIGN (or anti-CD55 or anti-CD46) and 10 μg/ml FITC-CTxB. Co-patching was induced by adding secondary Ab (Materials and methods), and, after fixation in PFA, cells were analyzed by confocal microscopy. Merged images are shown in the right panel. Results are representatives of multiple cells in three independent experiments. Bar, 5 μm.

membrane receptors transfected into K562, among which the β2-integrin LFA-1. Unlike DC-SIGN, LFA-1 molecules showed a random distribution pattern (unpublished data). It should be noted that the number of gold particles observed per micrometer squared was generally comparable with that observed for K-DC-SIGN, which should exclude difference in distribution due to major difference in the expression levels of the two receptors.

DC-SIGN predominantly resides in lipid rafts

To determine whether lipid rafts are important for DC-SIGN function, K-DC-SIGN cells were treated with methyl-β-cyclodextrin (MCD) to extract membrane cholesterol, and its effect on DC-SIGN–mediated ligand binding was tested by the fluorescent beads adhesion assay. As shown in Fig. 2 A, MCD treatment partially inhibits binding to gp120-coated beads, indicating that cholesterol extraction partially affected DC-SIGN ligand binding capacity.

To further demonstrate the association of DC-SIGN with lipid rafts, K-DC-SIGN cells were solubilized in Triton X-100 on ice and fractionated by centrifugation on a sucrose gradient at 4°C. With this procedure, lipid rafts, which can be isolated as detergent-resistant membranes (DRM), were recovered in low density fractions, whereas any other detergent-soluble material was concentrated in the high density fraction (Fig. 2 B). The GPI-anchored protein CD55 was used as the raft marker and was found in raft fractions, whereas the negative control (nonraft-associated protein), CD46, was almost completely detectable in the nonraft fractions. Similarly to CD55, a significant portion of DC-SIGN was recovered in the low density fraction, indicating that DC-SIGN is localized in DRM on the plasma membrane of K-DC-SIGN cells.

To provide further evidence that DC-SIGN colocalizes with lipid rafts, we examined the co-distribution of DC-SIGN and the lipid raft marker ganglioside (GM1), on K-DC-SIGN by antibody patching and confocal microscopy. As shown in Fig. 2 C, when capping was induced on K-DC-SIGN cells, GM1 clearly colocalizes with DC-SIGN and to the same extent as for CD55. However, some smaller patches of DC-SIGN were also detectable outside the lipid raft area, indicating that DC-SIGN might not permanently reside in lipid rafts, as also observed in Fig. 2 B. As expected, no colocalization of CD46 with GM1 was detected. Based on these observations, we conclude that DC-SIGN resides within a lipid raft environment on the plasma membrane of K-DC-SIGN cells.

DC-SIGN distribution changes during DC development

During the differentiation of DCs from monocyte precursors, the expression of DC-SIGN on the cell surface gradually increases (Geijtenbeek et al., 2000a). However, as shown by flow cytometry (Fig. 3 A), no significant increases in DC-SIGN expression levels are seen between cells harvested after 3 d of culture (designated intermediate DCs) and immature

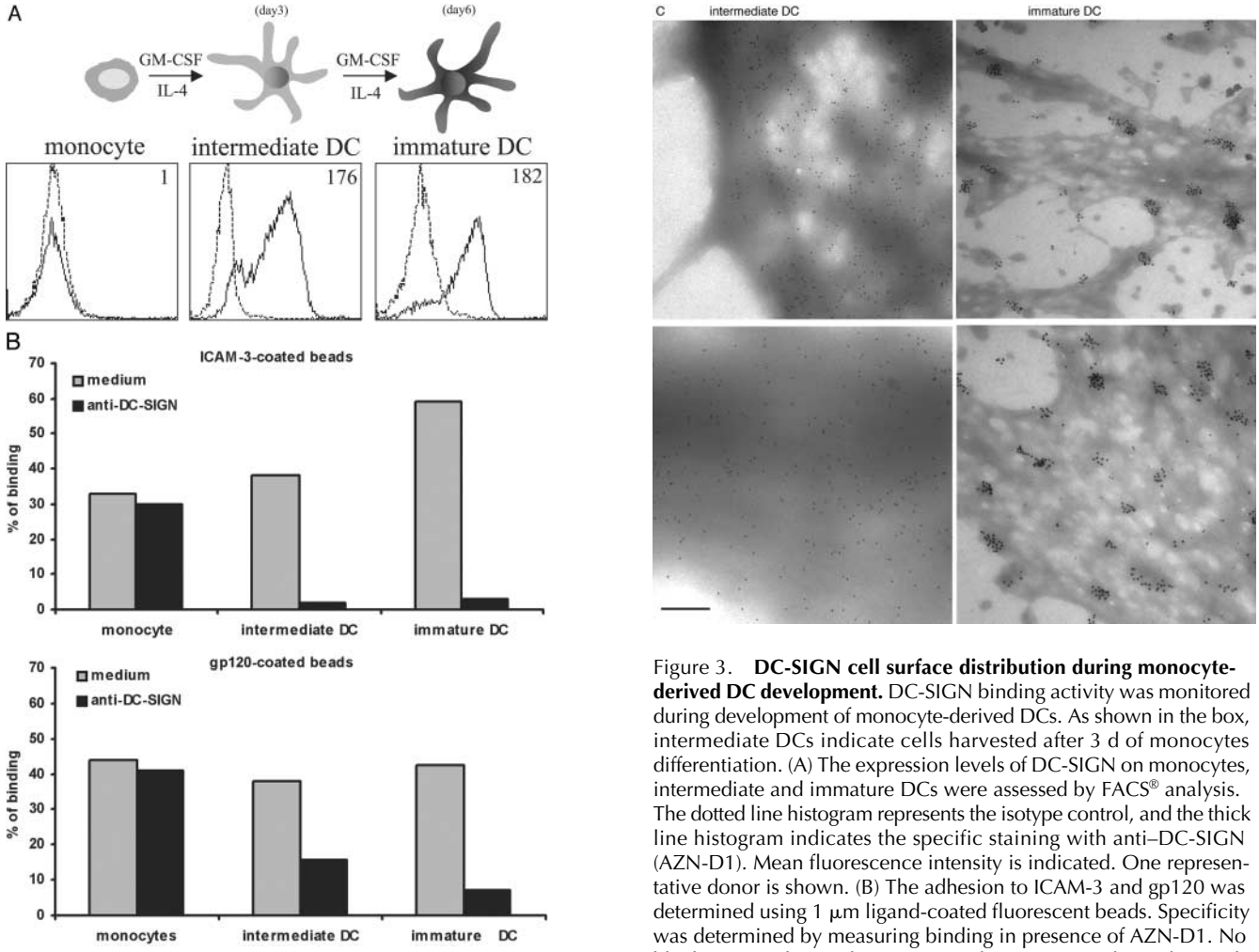

Figure 3. **DC-SIGN cell surface distribution during monocyte-derived DC development.** DC-SIGN binding activity was monitored during development of monocyte-derived DCs. As shown in the box, intermediate DCs indicate cells harvested after 3 d of monocytes differentiation. (A) The expression levels of DC-SIGN on monocytes, intermediate and immature DCs were assessed by FACS® analysis. The dotted line histogram represents the isotype control, and the thick line histogram indicates the specific staining with anti–DC-SIGN (AZN-D1). Mean fluorescence intensity is indicated. One representative donor is shown. (B) The adhesion to ICAM-3 and gp120 was determined using 1 μm ligand-coated fluorescent beads. Specificity was determined by measuring binding in presence of AZN-D1. No blocking was observed in presence of isotype control (not depicted). One representative experiments out of three is shown. (C) Intermediate and immature DCs were let adhere onto fibronectin-coated formvar film, specifically labeled for DC-SIGN with 10-nm gold particles (Materials and methods), and analyzed by TEM. Results are representatives of multiple cells in several independent experiments. Bar, 200 nm.

DCs. Maximum DC-SIGN–mediated adhesion to ICAM-3 as well as GP120 was observed on immature DCs, although already on intermediate DC DC-SIGN was capable of completely mediating the binding to ICAM-3 (Fig. 3 B, top), which on monocytes is LFA-1 dependent (unpublished data). Comparably, while on monocytes, binding to gp120 is mediated by CD4 (Kedzierska and Crowe, 2002; Kohler et al., 2003), on intermediate DCs, as well as on immature DCs, DC-SIGN is almost entirely responsible for binding to gp120 (Fig. 3 B, bottom). To examine DC-SIGN cell surface distribution, both intermediate and immature DCs were allowed to adhere to fibronectin, and DC-SIGN molecules were labeled with gold particles. Subsequently, the distribution on the plasma membrane was analyzed by TEM (Fig. 3 C). Given the high capacity of DCs to widely spread on the used substrates, very large membrane areas (often up to 60–70% of the whole visible plasma membrane) were available for gold particles analysis, ensuring that the areas used for quantitation were truly representative (Fig. S1, available at http://www.jcb.org/cgi/content/full/jcb.200306112/DC1). Surprisingly, we found that the distribution of DC-SIGN changes dramatically during DC development. Although on intermediate DCs, the gold particles are evenly distributed over the cell surface, on immature DCs, there is a clear organization of DC-SIGN in spatially well-defined microdomains. To exclude the possible influence of the fibronectin substrate on DC-SIGN distribution, TEM analysis was also performed on DCs that were gold labeled in suspension and mounted onto poly-L-lysine. No differences were seen between cells stretched on fibronectin or cells adhering to poly-L-lysine (unpublished data). Moreover, thin sections of resin-embedded immature DCs were gold labeled and analyzed by TEM. Clusters of DC-SIGN molecules could be observed exclusively at the plasma membrane (unpublished data). We also analyzed by TEM the cell surface distribution of other transmembrane receptors expressed on DCs, including LFA-1. Unlike DC-SIGN, LFA-1 did not show any changes in cell surface distribution pattern on intermediate and immature DCs (unpublished data).

To quantitatively describe the DC-SIGN distribution pattern, the nearest neighbor distance values among the gold particles were calculated applying a spatial-point pattern analysis. A quantitative comparison of DC-SIGN clustering among intermediate DCs, immature DCs, and K-DC-SIGN is shown in Fig. 4 A. On immature DCs, as well as on

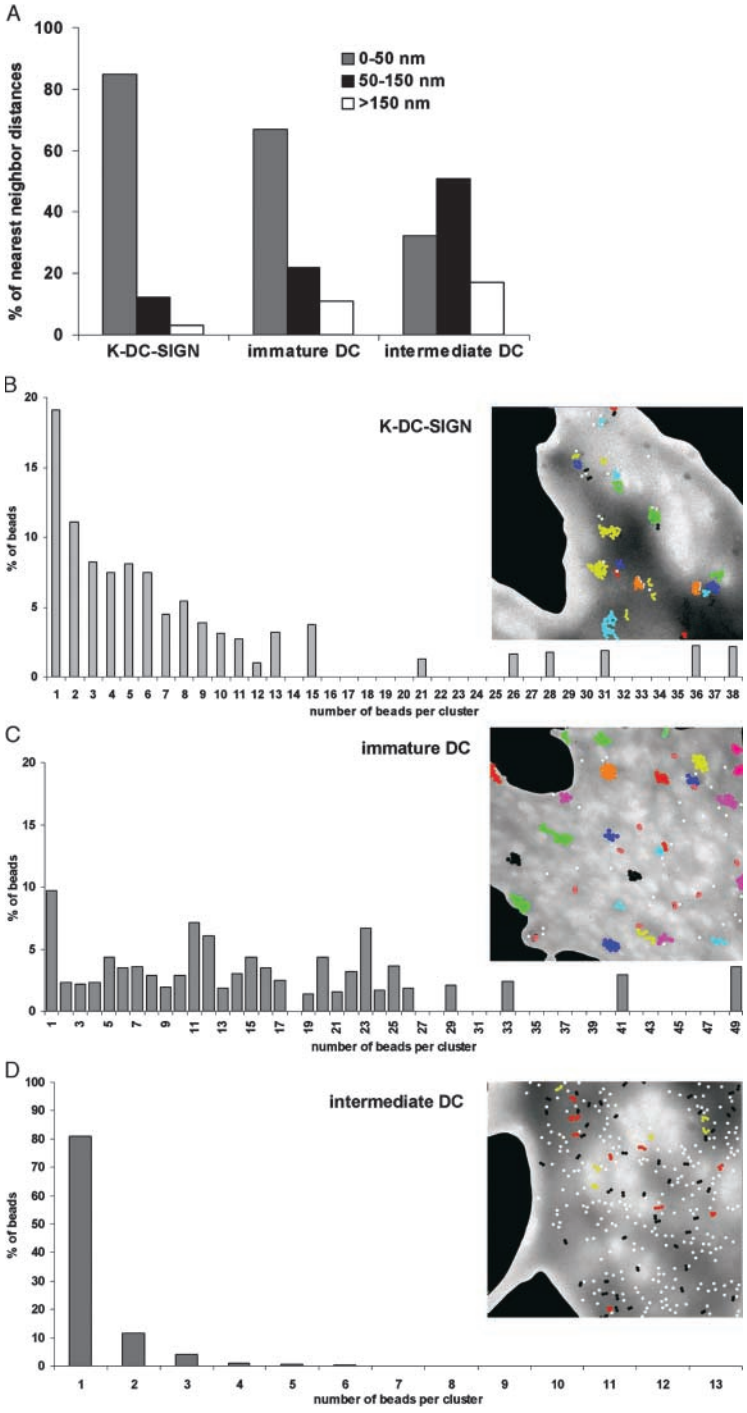

Figure 4. **Quantitative analysis of the distribution of gold particles labeling DC-SIGN.** The digital images of electron micrographs were processed by a custom-written software based on Labview. Gold labels were counted, and coordinates were assigned to each feature. Subsequently, interparticles distances were calculated using a nearest neighbor distance algorithm. Nearest neighbor distance values were calculated for each image, and the data of several independent experiments were pooled. Subsequently, the nearest neighbor distances were divided into three classes 0–50 nm (gray bar), 50–150 nm (black bar), and >150 nm (white bar), and the percentage of nearest neighbor distance values falling into each class was plotted (A). The partitioning of gold labels in clusters of various size (i.e.: number of particles/cluster) was also quantified. Clusters were defined when gold particles were <50 nm apart from a neighboring particle. The percentage of gold particles involved in the formation of a certain cluster size was calculated for (B) K-DC-SIGN, (C) immature DC, and (D) intermediate DC. The insets are three representative processed digital images, where each type of cluster is shown in a different color. For K-DC-SIGN, one representative experiment out of two is shown; for immature DC, one representative experiment out of six is shown; and for intermediate DCs, one representative experiment out of three is shown.

K-DC-SIGN, almost 70 and 80% of the gold particles reside within a 50-nm distance from its nearest neighbor, respectively. In contrast, on intermediate DCs, only 30% of the nearest neighbor distance values are found in the same category, and the majority of interparticle distances rather fall within the 50–150 nm range. It has to be noted that the intermediate and the immature DCs compared by spatial-point pattern analysis had a similar amount of gold particles per micrometer squared, confirming the comparable expression levels of DC-SIGN on the two cell types.

Similarly to what was observed for K-DC-SIGN, on immature DCs, these microdomains were also found to have an average diameter of ~200 nm and were separated from each other by an average distance of 400 nm. Spatial analysis of the microdomains distribution over the cell surface did not reveal any preferential localization in specific surface areas of the observed cells. These data were also confirmed by using high resolution near-field fluorescence imaging (unpublished data).

The relative partitioning of gold particles in clusters of various sizes (i.e., number of particles/cluster) was also quantified. A value of 50 nm was set to define the involvement of a gold particle in a cluster. Fig. 4 D shows that on intermediate DCs up to 80% of gold particles occur as single features. In contrast, on immature DCs (Fig. 4 C), as well as on

K-DC-SIGN (Fig. 4 B), DC-SIGN shows a much broader distribution of cluster sizes, with an average of 10–20 gold particles per cluster on immature DCs.

DC-SIGN resides in lipid rafts on DCs

Because, on K-DC-SIGN, we found a clear association of DC-SIGN with lipid rafts, we investigated whether DC-SIGN also colocalized with lipid rafts on immature DCs. Extraction of cholesterol by MCD resulted in a significant block in binding of both ICAM-3– and gp120-coated beads (Fig. 5 A). In contrast, DC-SIGN–mediated binding on intermediate DCs was not affected by cholesterol depletion (unpublished data).

To further demonstrate an interaction of DC-SIGN with lipid rafts on immature DCs, we investigated the co-distribution of DC-SIGN and GM1 by confocal microscopy. Fig. 5 B shows that, when capping was induced, DC-SIGN clearly colocalized with GM1, almost to the same extent as the raft marker CD55. However, similarly to what was observed on K-DC-SIGN, small patches of DC-SIGN were also found not colocalizing with GM1. To further prove the colocalization of GM1 with DC-SIGN, we performed double gold labeling for DC-SIGN and GM1 on immature DCs, and analyzed the samples by TEM. As shown in Fig. 5 C, GM1 (10 nm gold) was found within DC-SIGN microdomains (5 nm gold). Consistent with observations by confocal microscopy, some microdomains of DC-SIGN that lacked GM1 were also detected. Together, these results demonstrate that on immature DC DC-SIGN resides in microdomains that to a significant extent are associated with a lipid rafts environment.

DC-SIGN in microdomains facilitates binding to virus-sized particles

We showed that fluorescent beads coated with DC-SIGN–specific ligands were bound by immature as well as intermediate DCs, apparently independently of DC-SIGN organization on the cell membrane (Fig. 3, A and B).

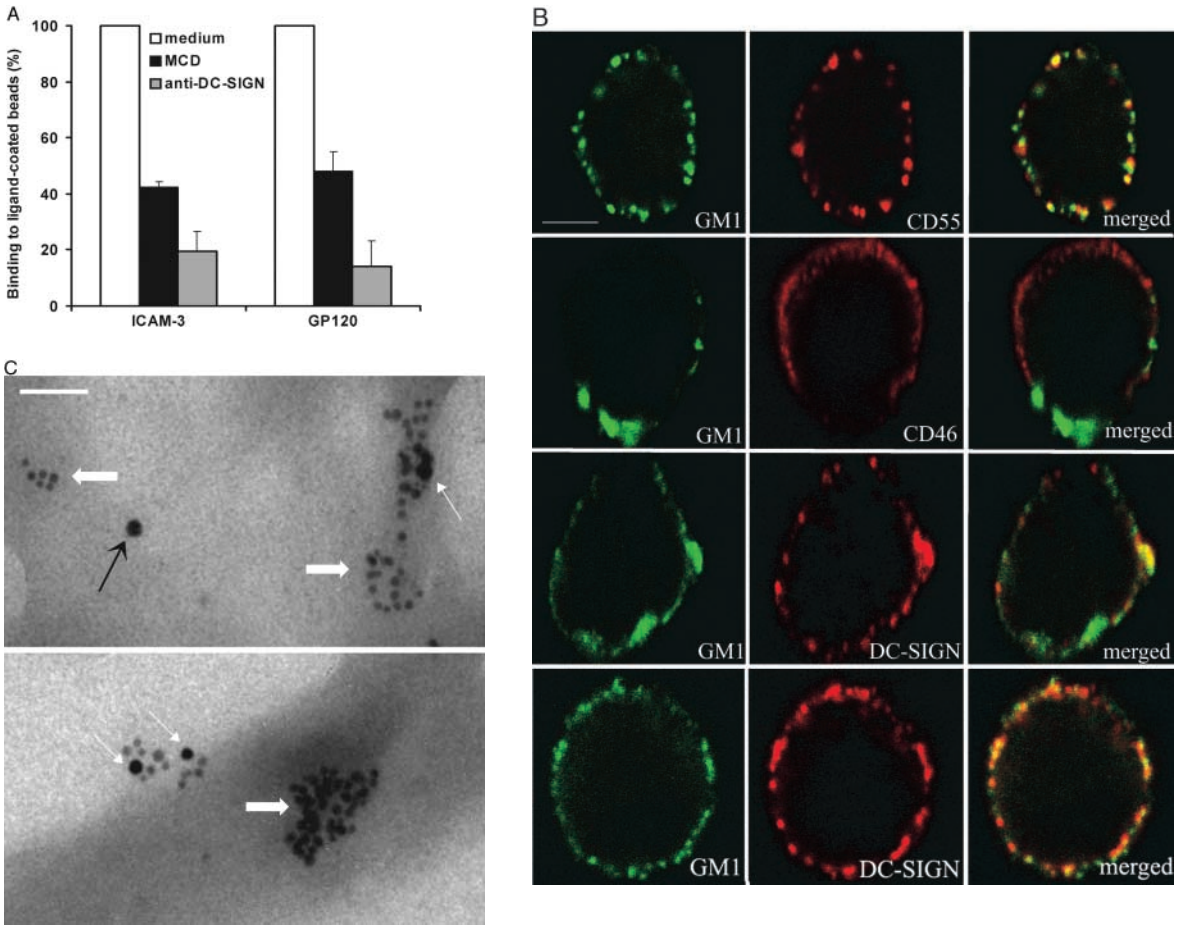

Figure 5. **DC-SIGN resides in lipid rafts on immature DCs.** (A) DC-SIGN–mediated adhesion to ligand-coated fluorescent beads (1-μm diam) on immature DCs was measured after cholesterol depletion by 20 mM MCD. The assay was performed as described in Fig. 2 A. Data shown are means ± SD of one representative experiment performed in triplicate out of three. One representative experiment out of three is shown. (B) Confocal microscopy analysis of copatching of DC-SIGN and GM1 on immature DCs. Staining was performed as described in Fig. 2 C. Cells were analyzed by confocal microscopy. Merged images are shown in the right panel. Results are representative of multiple cells in two independent experiments. Bar, 5 μm. (C) Whole-mount samples of immature DCs were double labeled for DC-SIGN (5 nm gold) and the raft marker GM1 (10 nm gold) and analyzed by TEM. Thin white arrows indicate GM1 colocalizing in DC-SIGN microdomains. Thick white arrows indicate DC-SIGN microdomains with no GM1. Black arrow indicates GM1 alone. Results are representatives of multiple cells in two independent experiments. Bar, 50 nm.

However, because DC-SIGN on immature DCs is an exquisite virus receptor and the fluorescent beads are at least one order of magnitude larger than viral particles, we investigated whether clustering of DC-SIGN into higher order assemblies might be needed to stabilize interactions with virus-sized particles. To detect possible differences in "avidity" for multimeric ligands between scattered and clustered DC-SIGN molecules, and to mimic virus binding to DC-SIGN, we used fluorescent virus-sized microbeads of 40-nm diam, coated with gp120, which are now referred to as virus-sized particles. The extremely broad fluorescence emission peak of these microbeads currently precludes accurate quantification by flow cytometry, therefore binding of DCs to these virus-sized particles was visualized by confocal microscopy.

When comparing the capacity of intermediate and immature DCs to bind these virus-sized particles (Fig. 6), a very high binding was observed on immature DCs. Many virus-sized particles were bound to the plasma membrane and a significant amount was phagocytosed (Fig. 6, D and E). In contrast, intermediate DCs (Fig. 6, A and B) hardly bound any microbeads, comparable to background levels or when DCs were pretreated with the carbohydrate mannan to block DC-SIGN (Fig. 6, C and F). Similar results were obtained when microbeads coated with ICAM-3 were used (unpublished data). Moreover, DC-SIGN on intermediate as well as on immature DCs was found to be equally capable of binding to soluble recombinant gp120 (Fig. 6 G), suggesting that the intrinsic binding capacity of DC-SIGN molecule on the two different DC types is comparable. Similar results were obtained when soluble ICAM-3-Fc chimeras were used (unpublished data). All these observations support our hypothesis that DC-SIGN molecules acquire a higher avidity for multimeric ligands when organized in multimolecular assemblies.

DC-SIGN microdomains enhances HIV-1 infection

Having established that DC-SIGN microdomains bind virus-sized particles more efficiently in comparison to randomly distributed receptor molecules, we investigated whether the uptake of real virus was also enhanced by a clus-

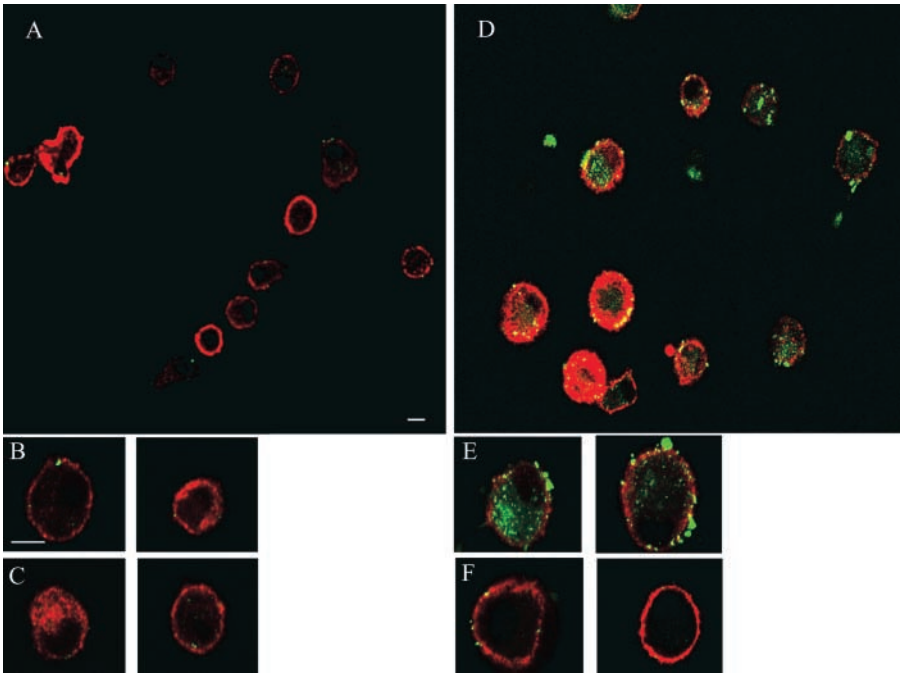

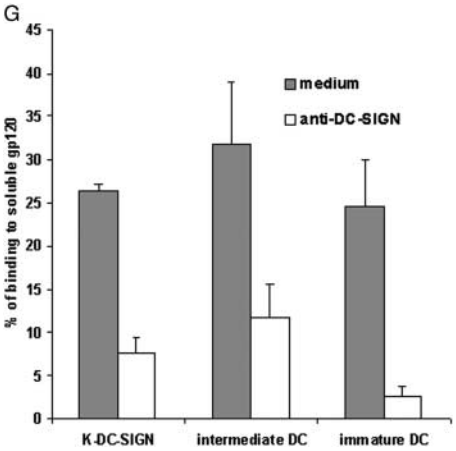

Figure 6. **DC-SIGN microdomains on immature DCs bind virus-sized particles.** Green fluorescent microbeads (40-nm diam) were coated with gp120 and added to the cells in a ratio of 20 beads/cell. The cells were incubated for 30 min at 37°C, washed, and fixed in PFA. DC-SIGN was stained with AZN-D1 and Alexa 647–conjugated goat anti–mouse Ab (red). Subsequently, the cells were mounted onto poly-L-lysine–coated glass coverslips and analyzed by confocal microscopy. The overview of binding to gp120 microbeads of (A) intermediate DCs and (D) immature DCs is shown. Two representative cells of (B) intermediate and (E) immature DCs are shown. Specific block with 100 μg/ml mannan was also performed by preincubating the cells at RT for 10 min before adding the microbeads (C and F); bars, 5 μm. Similar results were obtained with ICAM-3–coated microbeads (not depicted). (G) Binding of K-DC-SIGN, intermediate DCs, and immature DCs to soluble gp120 was also performed: 50,000 cells were incubated with 50 mM biotinylated gp120 for 30 min on ice, in presence or absence of 20 μg/ml anti–DC-SIGN blocking mAb (AZN-D1). A subsequent incubation with Alexa 488–conjugated streptavidin for 30 min on ice followed, and gp120 molecules bound to the cells were detected by flow cytometry. The values represent the mean of three independent experiments ±SD.

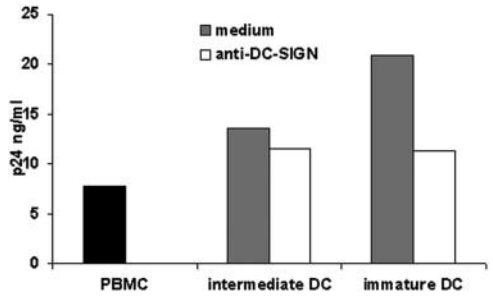

Figure 7. **Clustered DC-SIGN molecules efficiently bind HIV-1 particles and infect PBMC.** DC-SIGN on immature DCs enhances HIV-1 infection as measured in a DC-PBMC coculture. Either intermediate or immature DCs (1.5×10^6) were preincubated for 20 min at RT with or without blocking mAb against 20 μg/ml DC-SIGN (AZN-D1 and AZN-D2). Preincubated intermediate or immature DCs were pulsed for 2 h with HIV-1 (M-tropic HIV-1Ba-L strain), and unbound virus particles and mAb were washed away. Subsequently, DCs were cocultured with activated PBMC (1.5×10^6) for 7 d. Coculture supernatants were collected, and p24 antigen levels were measured by ELISA. Black histogram represents PBMC infected in the absence of DCs. One representative experiment out of two is shown.

tered distribution of DC-SIGN, using p24 ELISA. Therefore, intermediate and immature DCs were pulsed for 2 h with HIV-1 (M-tropic HIV-1Ba-L strain), washed, and cultured in the presence of activated peripheral blood mononuclear cells (PBMC). As shown in Fig. 7, virus replication was significantly higher when PBMC were cocultured with either intermediate or immature DCs with respect to PBMC alone challenged with the same amount of infectious virus. However, infection of PBMC cultured with virus-pulsed immature DCs was much higher than the infection exhibited by PBMC cultured with intermediate DCs. In addition, the infection of PBMC with immature DCs was significantly blocked by anti–DC-SIGN mAbs that were added to DCs before incubation with HIV-1. In contrast, DC-SIGN contribution to PBMC infection was clearly much lower when intermediate DCs were used. The incomplete blocking observed in the presence of anti–DC-SIGN Abs suggests the involvement of other HIV receptors also expressed on DCs (Turville et al., 2002). The comparable expression levels of DC-SIGN, as shown in Fig. 3 A, as well as several costimulatory molecules (such as CD40 and CD80) on intermediate and immature DCs suggest that these two DC types have similar antigen presentation capacity (unpublished data). Altogether, our data demonstrate that DC-SIGN organized in microdomains rather than randomly distributed is more efficient in mediating binding and uptake of virus-sized microbeads as well as real HIV-1 particles.

Discussion

DC-SIGN is a DC-specific C-type lectin that acts both as adhesion molecule and as pathogen-recognition receptor. Here, we demonstrate that DC-SIGN can form microdomains on the plasma membrane, and that there is a direct correlation between the distribution of DC-SIGN in microdomains and its capacity to bind and internalize virus-sized ligand-coated particles. Moreover, to the best of our knowledge, this is the first report describing a C-type lectin in a lipid raft environment on DCs that forms highly organized well-defined (200 nm) multiprotein assemblies on the surface of a cell.

To establish the association of proteins with lipid rafts is complicated and often controversial, which underscores the complexity of cell membranes. These lipid domains differ in their composition, physical properties, and biological functions (Schuck et al., 2003). Moreover, lipid raft compositions differ between cell types. Finally, the dynamics of the chemical membrane composition adds a further level of complexity. Therefore, the association of proteins with lipid rafts can only be analyzed using different techniques simultaneously. Our observation that DC-SIGN resides within lipid rafts is based on several well-established raft analysis techniques. First, we showed by biochemical experiments the partitioning of DC-SIGN in DRM. Second, co-patching of DC-SIGN with the lipid raft marker GM1 was observed by confocal microscopy. Third, this association between DC-SIGN and GM1 was confirmed by TEM. Fourth, cholesterol extraction by MCD inhibited DC-SIGN–mediated binding. Surprisingly, on immature DCs, the same MCD treatment did not have any effect on the organization of DC-SIGN microdomains, as observed by TEM (unpublished data). This may be explained by the fact that the remaining cholesterol may be sufficient to keep such domains intact (Schuck et al., 2003). Moreover, besides cholesterol, also glycosphingolipids, another lipid raft component, which is not depleted by MCD treatment, may in part maintain the integrity of DC-SIGN microdomains. The fact that cholesterol extraction by MCD partially affects DC-SIGN–mediated binding could be explained by considering the pleiotropic effects that MCD can have on cell functions, besides disrupting lipid rafts integrity (Brown and London 2000; Edidin 2001; Schuck et al., 2003). Therefore, MCD treatment can only be a preliminary indicator for a possible association of a protein with a lipid rafts environment. Also, it should be added that, unlike for GPI-anchored proteins, very little is known about how transmembrane proteins are recruited into lipid rafts, how stable these interactions are and what exactly the role of cholesterol is. Further experiments are needed to better identify the molecular determinants that control the association of transmembrane proteins with lipid rafts.

In vitro experiments with isolated recombinant C-type lectins suggested that these can oligomerize providing multiple surfaces to bind (multivalent) ligands (Drickamer, 1999). DC-SIGN has been shown to form tetramers stabilized by an α-helical stalk (Mitchell et al., 2001), and purified truncated forms of DC-SIGN containing the complete ECD were also shown to be able to bind ligands by surface plasmon resonance (Lozach et al., 2003). In these works, the affinity of isolated CRDs or complete ECDs of DC-SIGN for the ligand was measured and compared with the affinity of the membrane-bound form. Although no interactions with the ligand could be found using isolated CRDs, significant binding was detected if single CRDs were closely seeded ($K_d = 48$ nM) or if CRDs were part of a complete oligomeric-soluble ECD of DC-SIGN ($K_d = 30$ nM). The highest affinity was seen with membrane-bound DC-SIGN expressed on the surface of transfected cells ($K_d = 3$ nM), suggesting that the nat-

ural plasma membrane environment strongly influences the function of this receptor. To some extent, this mirrors our observations: DC-SIGN on the cell surface of intermediate DCs is randomly distributed and hardly binds virus-sized particles, whereas on immature DCs, the protein is organized in well-defined microdomains, which allows binding of 40-nm virus-sized particles (Fig. 6, A–F). In apparent contrast, we showed that on intermediate DCs, randomly distributed DC-SIGN was able to bind 1-μm beads, coated with ICAM-3 or gp120 (Fig. 3 B). This apparent discrepancy between 40-nm virus-sized particles and 1-μm beads can be explained by the fact that beads of 1-μm diam have ~600-fold larger interaction surface saturated with numerous ligand molecules that can engage simultaneous interactions with several individual DC-SIGN molecules. These multiple interactions may signal into the cell and lead to a rapid recruitment of new DC-SIGN molecules, thus strengthening the binding. In contrast, when virus-sized particles are used, the contact surface and therefore, the number of ligand molecules is much smaller. Consequently, only interactions with DC-SIGN molecules in highly organized multiprotein assemblies can result in stable binding of virus-sized particles (Fig. 8). When a computer-aided simulation was performed to predict the capacity of round objects of different sizes to establish interactions with either random or clustered DC-SIGN molecules, we found that objects with a diameter in the range of virus sizes (40–200-nm diam) preferentially bind to clusters of DC-SIGN having the same size (unpublished data). In agreement with this model, no significant differences were detected in binding of intermediate and immature DCs to soluble gp120 or to ICAM-3-Fc chimeras, indicating that the capacity of each single DC-SIGN molecule to recognize and bind the ligand is comparable on both DC types (Fig. 6 G).

The biological relevance of this clustering phenomenon is shown by the fact that immature DCs compared with intermediate DCs showed an enhanced DC-SIGN–mediated binding and internalization of virus particles, and subsequent infection of PBMC in trans (Fig. 7). Therefore, we propose that engagement of viruses with DC-SIGN occurs much more productively when this receptor is organized in microdomains and resides in a lipid raft or cholesterol-enriched environment.

It remains to be established what controls DC-SIGN random distribution on intermediate DCs and what mechanism is responsible for the change into a clustered organization on immature DCs. We cannot exclude that, on intermediate DCs, DC-SIGN may interact with an unknown membrane associated protein that prevents the formation of such microdomains. Alternatively, cytoskeletal constraints may differ between these cells, and this issue is currently under investigation. Preliminary observations suggest that releasing DC-SIGN molecules from the cortical actin cytoskeleton by cytochalasin D treatment results in an enhanced ligand binding, particularly on intermediate DCs (unpublished data). Further experiments are needed to obtain insight into the formation of DC-SIGN multiprotein assemblies on DCs.

DC-SIGN belongs to the C-type lectin family that, together with the TLR family, forms the first barrier against invading pathogens. This occurs through recognition of pathogen-associated molecular patterns displayed at the cell surface of microorganisms. Although TLRs have been shown to induce differential gene expression upon recognition of distinct pathogen structural components (Akira, 2003), for the C-type lectins, and particularly for DC-SIGN, no direct signaling pathways has been demonstrated so far. Therefore, it will be interesting to investigate the interactions that might occur between these two families of pathogen-recognition receptors.

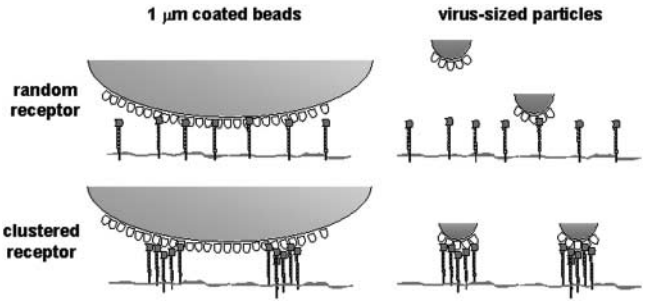

Figure 8. **DC-SIGN microdomains enhances binding of virus-sized particles with respect to isolated DC-SIGN molecules.** Beads of 1-μm diam are saturated with numerous coated ligand molecules that can engage simultaneous interactions with several individual DC-SIGN molecules. These multiple interactions may strengthen the binding both with random and clustered DC-SIGN. In contrast, when virus-sized particles are used, the contact surface and therefore, the number of ligand molecules is much smaller. Consequently, only interactions with DC-SIGN molecules in highly organized multiprotein assemblies may result in stable binding of virus particles.

In conclusion, our findings emphasize the importance of relating the function with the cell surface organization of DC-SIGN. Clustered distribution is essential to enhance the interaction as well as the internalization efficiency of DC-SIGN–pathogen complexes. In addition, our data highlight the importance of the plasma membrane as a specialized microenvironment, where finely orchestrated interactions among proteins, carbohydrates, and lipids take place. These complex interactions mediate many fundamental processes that occur at the contact site between cells (cell–cell or cell–pathogen), such as assembly of signaling platforms and formation of entry portals for invasive pathogens.

Insight in the cell surface organization of pathogen scavenger receptors like DC-SIGN will contribute to the development of novel strategies that specifically inhibit interactions with life-threatening pathogens like HIV-1 or *Mycobacterium.*

Materials and methods

Antibodies and reagents

For labeling as well as blocking of DC-SIGN, the mAb AZN-D1 was used (Geijtenbeek et al., 2000a). For detection of CD46 and CD55 the Abs E4.3 (BD Biosciences) and 143–30 (CLB) were used, respectively. Alexa 647–conjugated goat anti–mouse IgG was purchased from Molecular Probes. FITC-conjugated cholera toxin B subunit (FITC-CTxB), Triton X-100, and MCD were purchased from Sigma-Aldrich. Goat anti-CTxB antibody was purchased from Calbiochem.

Cells

Monocytes were obtained from buffy coats of healthy individuals and were purified using Ficoll density centrifugation. Immature DCs were obtained as reported elsewhere (Geijtenbeek et al., 2000a). In brief, DCs were cul-

tured from monocytes in presence of IL-4 and GM-CSF (500 and 800 U/ml, respectively) for 3 d to obtain intermediate DCs and for 6 d to obtain immature DCs. Stable K562 transfectants expressing DC-SIGN (K-DC-SIGN) were generated as published previously (Geijtenbeek et al., 2000a).

Adhesion assays

Carboxylate-modified TransFluorSpheres (488/645 nm, 1-μm diam; Molecular Probes) were coated with ICAM-3-Fc or GP120, and the fluorescent beads adhesion assay was performed as described previously (Geijtenbeek et al., 1999). When the lipid raft-disrupting agent MCD was used, the cells were resuspended in serum-free medium containing the appropriate concentration of MCD and preincubated for 30 min at 37°C. When necessary, 50,000 cells were incubated with 20 μg/ml blocking mAb for 10 min at RT. The ligand-coated fluorescent beads (20 beads/cell) were added and the suspension was incubated for 30 min at 37°C. Adhesion was determined by measuring the percentage of cells, which have bound fluorescent beads, by flow cytometry using the FACSCalibur™ (Becton Dickinson). Streptavidin-modified TransFluorSpheres (505/515 nm, 40-nm diam; Molecular Probes) were coated with ICAM-3-Fc or GP120 as described previously for 1-μm beads (Geijtenbeek et al., 1999) and were added to DCs in a ratio of ~20 beads/cell. Bound beads were detected by confocal microscopy analysis of the cells.

When binding to soluble GP120 was performed, 50 mM biotinylated GP120 was added to the cells (10^5) for 30 min on ice, in presence or absence of 20 μg/ml anti–DC-SIGN blocking Ab (AZN-D1). After the incubation, cells were extensively washed and incubated with Alexa 488–conjugated streptavidin for 30 min on ice. Subsequently, bound GP120 molecules were detected by flow cytometry.

Labeling procedures

For flow cytometry analysis, cells were incubated (30 min; 4°C) in PBA (PBS, containing 0.5% BSA and 0.01% sodium azide), with different mAb (5 μg/ml), followed by incubation with FITC-labeled goat anti–mouse IgG antibody (GAM-FITC; Zymed Laboratories; 1:50 dilution in PBA) for 30 min at 4°C. The relative fluorescence intensity was measured on a FACSCalibur™. Isotype–specific controls were included. For TEM, K-DC-SIGN were fixed onto poly-L-lysine–coated formvar, whereas DCs were allowed to spread on glass coverslips covered by a thin layer of fibronectin-coated formvar for 1 h at 37°C and immediately fixed with 1% PFA for 15 min. After two washing steps with PBS and a subsequent incubation (60 min at RT) with I-buffer (PBS, 0.1% glycine, 1% BSA, and 0.25% gelatin) to reduce a specific background, the specimens were incubated for 30 min with the primary antibodies in I-buffer on ice, rinsed in PBS, and fixed in 1% PFA and 0.1% glutaraldehyde for 15 min. After two washing steps with PBS and a block in I-buffer, the samples were incubated with rabbit anti–mouse IgG (to detect mAb) for 30 min on ice. A final incubation with 10-nm-diam gold-labeled Protein A (to detect polyclonal antibodies) was performed, followed by final fixation in 1% glutaraldehyde in phosphate buffer for 20 min at RT. When double labeling was performed, the cells were treated as described above, except that anti–DC-SIGN (AZN-D1), and biotinylated-CTxB were added simultaneously; and finally, goat anti–mouse-conjugated 5-nm gold and streptavidin-conjugated 10-nm gold were used to label DC-SIGN and GM1, respectively. Isotype-specific controls were always included. The 10-nm-diam gold-labeled protein A was a gift of M. Wijers and H. Croes (Nijmegen Center for Molecular Life Sciences). The goat anti–mouse-conjugated 5-nm gold and streptavidin-conjugated 10-nm gold were purchased from Aurion.

EM and analysis of the distribution patterns of gold particles

After gold labeling and fixation, the specimens were dehydrated by sequential passages through 30, 50, 70, 90%, and absolute ethanol. Next, the ethanol was substituted by liquid CO_2, and the samples were critical point dried. The formvar films were transferred from the glass onto copper grids, and the specimens were observed in a transmission electron microscope (model 1010; JEOL), operating at 60–80 kV. Gold particles were detected on the periphery and thinner parts of cells, where a good contrast could be achieved. In case of DCs, which widely spread (Fig. S1), the membrane area available for analysis represented up to 60–70% of the whole labeled plasma membrane. For each cell at least four to six areas were analyzed at random. The digital images of electron micrographs were processed by custom-written software based on Labview (National Instruments). The distribution pattern of DC-SIGN (i.e., the degree of clustering) was analyzed by counting the number of gold particles found on the plasma membrane in a semi-automatic fashion. Subsequently, coordinates were assigned to the observed beads and interparticles distance statistics were obtained using a nearest neighbor distance algorithm. Clusters were defined when gold particles were less than a set distance apart from a neighboring particle.

Confocal microscopy

Cells were stained at 4°C with 10 μg/ml anti–DC-SIGN antibody (AZN-D1), anti-CD55 antibody, anti-CD46 antibody, and 10 μg/ml FITC-CTxB. Isotype-specific controls were always included. Secondary staining for DC-SIGN, CD55, and CD46 was with Alexa 647–conjugated goat anti–mouse IgG, and for FITC-CTxB with goat anti-CTxB. Patching was induced by incubation at 12°C for 1 h, followed by fixation with 1% PFA. Cells were mounted onto poly-L-lysine–coated glass coverslips. Signals were collected sequentially to avoid bleed through.

Detergent extraction and flotation assay

For detergent resistant membrane isolation, K-DC-SIGN cells (10×10^6) were lysed on ice in 0.5 ml of lysis buffer (50 mM Tris, pH 7.4, 150 mM NaCl, 5 mM EDTA, and 1% Triton X-100, plus a cocktail of protease inhibitors: 1 mM PMSF, 10 μg/ml aprotinin, and 10 μg/ml leupeptin). After 30 min of incubation, the lysate was made 40% with respect to sucrose. Next, the lysate-sucrose mixture was overlaid with 2 ml of 30% sucrose in lysis buffer and finally with 1 ml of 4% sucrose in lysis buffer. The mixture was centrifuged at 200,000 *g* for 14–16 h in an SW60Ti rotor (Beckman Coulter). The gradient was fractionated in 0.5-ml fractions from the bottom of the tube.

Immunoblot analysis

Proteins from the sucrose fractions were separated by SDS-PAGE and transferred to PROTRAN nitrocellulose transfer membranes (Schleicher & Schuell). Membranes were blocked for 1 h at RT using 2% nonfat dried milk (Campina) and 1% BSA (Calbiochem) in 0.1% PBS/Tween 20. Blots were subsequently incubated with specific antibodies (polyclonal anti-CD55 and CD46 from Santa Cruz Biotechnology, Inc., and a polyclonal anti–DC-SIGN antibody [CSRD] that was raised in our laboratory), followed by the appropriate HRP-conjugated secondary antibodies (DakoCytomation). Finally, proteins were detected using ECL (Amersham Biosciences).

HIV-1 infection of DCs

Infection of intermediate and immature DCs with the M-tropic strain HIV-1Ba-L was performed as described previously (Geijtenbeek et al., 2000b). In brief, intermediate and immature DCs (1.5×10^6) were incubated with mAb against 20 μg/ml DC-SIGN (AZN-D1 and 20 μg/ml AZN-D2 for 20 min at RT. Subsequently, cells were incubated with the M-tropic strain HIV-1Ba-L for 2 h with a multiplicity of infection of 0.004. After incubation, cells were washed and cocultured with activated PBMC in the presence of 5 U/ml human recombinant IL-2 (Roche Diagnostics). PBMC were activated by culturing them before infection for 3 d in the presence of 2 μg/ml of phyto-HA (Sigma-Aldrich). After 7 d, culture supernatants were collected, and p24 antigen levels were determined by a p24 antigen ELISA (AMPAK™; DakoCytomation).

Online supplemental material

Fig. S1 is an overview of DC whole-mount samples by TEM. To determine the organization of DC-SIGN on the cell membrane at high resolution, TEM was used on whole-mount samples of intermediate as well as immature DCs, after specific labeling with anti–DC-SIGN mAb and 10-nm gold particles. It should be noted that the specimens were not sectioned, thus, making the whole cell surface available for gold labeling and subsequent TEM analysis. DCs were adhered onto fibronectin-coated formvar film, fixed, and labeled as described in Materials and methods, and finally analyzed by TEM. Given the high capacity of both intermediate and immature DCs to widely spread on the substrate, very large membrane areas (often up to 60–70% of the whole visible plasma membrane) were available for gold particles analysis, ensuring that the areas used for quantitation were truly representative. One representative overview of DCs on fibronectin-coated formvar is shown. Bar, 6 μm. Online supplemental material is available at http://www.jcb.org/cgi/content/full/jcb.200306112/DC1.

This work is dedicated to the loving memory of Hans Smits.

We thank Mietske Wijers and Huib Croes for providing gold beads and for their help with electron microscopy and W.J. de Grip for biochemistry facility. We also acknowledge Rob Schuurman for his help with the p24 ELISA. We are also grateful to Maria Garcia-Parajo, Gosse Adema, and Ruurd Torensma for critical reading of the manuscript.

A. Cambi is supported by a grant SLW 33.302P from the Netherlands Organization of Scientific Research, Earth and Life Sciences. F. de Lange is supported by a grant FB-N/T-1a from the Netherlands Foundation for Fun-

damental Research of Matter. C.G. Figdor is supported by grant NWO 901-10-092.

Submitted: 20 June 2003
Accepted: 7 November 2003

References

Akira, S. 2003. Mammalians Toll-like receptors. *Curr. Opin. Immunol.* 15:5–11.

Alvarez, C.P., F. Lasal, J. Carrillo, O. Muniz, A.L. Corbi, and R. Delgado. 2002. C-type lectins DC-SIGN and L-SIGN mediate cellular entry by Ebola virus in cis and in trans. *J. Virol.* 76:6841–6844.

Banchereau, J., and R.M. Steinman. 1998. Dendritic cells and the control of immunity. *Nature.* 392:245–252.

Brown, D.A., and E. London. 2000. Structure and function of sphingolipid- and cholesterol-rich membrane rafts. *J. Biol. Chem.* 275:17221–17224.

Cambi, A., K. Gijzen, I.J.M. de Vries, R. Torensma, B. Joosten, G.J. Adema, M.G. Netea, B.J. Kullberg, L. Romani, and C.G. Figdor. 2003. The C-type lectin DC-SIGN (CD209) is an antigen-uptake receptor for *Candida albicans* on dendritic cells. *Eur. J. Immunol.* 33:532–538.

Colmenares, M., A. Puig-Kroger, O.M. Pello, A.L. Corbi, and L. Rivas. 2002. Dendritic cell (DC)-specific intercellular adhesion molecule 3 (ICAM-3)-grabbing nonintegrin (DC-SIGN, CD209), a C-type surface lectin in human DCs, is a receptor for *Leishmania* amastigotes. *J. Biol. Chem.* 277: 36766–36769.

Dimitrov, D.S. 1997. How do viruses enter cells? The HIV coreceptors teach us a lesson of complexity. *Cell.* 91:721–730.

Drickamer, K. 1999. C-type lectin-like domains. *Curr. Opin. Struct. Biol.* 9:585–590.

Edidin, M. 2001. Shrinking patches and slippery rafts: scales of domains in the plasma membrane. *Trends Cell Biol.* 11:492–496.

Figdor, C.G., Y. van Kooyk, and G.J. Adema. 2002. C-type lectin receptors on dendritic cells and Langerhans cells. *Nat. Rev. Immunol.* 2:77–84.

Gatfield, J., and J. Pieters. 2000. Essential role for cholesterol in entry of mycobacteria into macrophages. *Science.* 288:1647–1650.

Geijtenbeek, T.B., Y. van Kooyk, S.J. van Vliet, M.H. Renes, R.A. Raymakers, and C.G. Figdor. 1999. High frequency of adhesion defects in B-lineage acute lymphoblastic leukemia. *Blood.* 94:754–764.

Geijtenbeek, T.B., R. Torensma, S.J. van Vliet, G.C. van Duijnhoven, G.J. Adema, Y. van Kooyk, and C.G. Figdor. 2000a. Identification of DC-SIGN, a novel dendritic cell-specific ICAM-3 receptor that supports primary immune responses. *Cell.* 100:575–585.

Geijtenbeek, T.B., D.S. Kwon, R. Torensma, S.J. van Vliet, G.C. van Duijnhoven, J. Middel, I.L. Cornelissen, H.S. Nottet, V.N. Kewal Ramani, D.R. Littman, et al. 2000b. DC-SIGN, a dendritic cell-specific HIV-1-binding protein that enhances trans-infection of T cells. *Cell.* 100:587–597.

Geijtenbeek, T.B., D.J. Krooshoop, D.A. Bleijs, S.J. van Vliet, G.C. van Duijnhoven, V. Grabovsky, R. Alon, C.G. Figdor, and Y. van Kooyk. 2000c. DC-SIGN-ICAM-2 interaction mediates dendritic cell trafficking. *Nat. Immunol.* 1:353–357.

Geijtenbeek, T.B., S.J. van Vliet, E.A. Koppel, M. Sanchez-Hernandez, C.M. Vandenbroucke-Grauls, B. Appelmelk, and Y. van Kooyk. 2003. Mycobacteria target DC-SIGN to suppress dendritic cell function. *J. Exp. Med.* 197:7–17.

Halary, F., A. Amara, H. Lortat-Jacob, M. Messerle, T. Delaunay, C. Houles, F. Fieschi, F. Arenzana-Seisdedos, J.F. Moreau, and J. Dechanet-Merville. 2002. Human cytomegalovirus binding to DC-SIGN is required for dendritic cell infection and target cell trans-infection. *Immunity.* 17:653–664.

Kedzierska, K., and S.M. Crowe. 2002. The role of monocytes and macrophages in the pathogenesis of HIV-1 infection. *Curr. Med. Chem.* 9:1893–1903.

Kogelberg, H., and T. Feizi. 2001. New structural insights into lectin-type proteins of the immune system. *Curr. Opin. Struct. Biol.* 11:635–643.

Kohler, J.J., D.L. Tuttle, C.R. Coberley, J.W. Sleasman, and M.M. Goodenow. 2003. Human immunodeficiency virus type 1 (HIV-1) induces activation of multiple STATs in CD4+ cells of lymphocyte or monocyte/macrophage lineages. *J. Leukoc. Biol.* 73:407–416.

Lafont, F., G. Tran van Nhieu, K. Hanada, P. Sansonetti, and F.G. van der Groot. 2002. Initial steps of Shigella infection depend on the cholesterol/sphingolipid raft-mediated CD44-IpaB interaction. *EMBO J.* 21:4449–4457.

London, E., and D.A. Brown. 2000. Insolubility of lipids in triton X-100: physical origin and relationship to sphingolipid/cholesterol membrane domains (rafts). *Biochim. Biophys. Acta.* 1508:182–195.

Lozach, P.Y., H. Lortat-Jacob, A. De Lacroix De Lavalette, I. Staropoli, S. Foung, A. Amara, C. Houles, F. Fieschi, O. Schwartz, J.L. Virelizier, et al. 2003. DC-SIGN and L-SIGN are high-affinity binding receptors for hepatitis C virus glycoprotein E2. *J. Biol. Chem.* 278:20358–20366.

Maeda, N., J. Nigou, J.L. Herrmann, M. Jackson, A. Amara, P.H. Lagrange, G. Puzo, B. Gicquel, and O. Neyrolles. 2003. The cell surface receptor DC-SIGN discriminates between *Mycobacterium* species through selective recognition of the mannose caps on lipoarabinomannan. *J. Biol. Chem.* 278: 5513–5516.

Mahnke, K., M. Guo, S. Lee, H. Sepulveda, S.L. Swain, M. Nussenzweig, and R.M. Steinman. 2000. The dendritic cell receptor for endocytosis, DEC-205, can recycle and enhance antigen presentation via major histocompatibility complex class II-positive lysosomal compartments. *J. Cell Biol.* 151: 673–684.

Mañes, S., G. del Real, R.A. Lacalle, P. Lucas, C. Gomez-Mouton, S. Sanchez-Palomino, R. Delgado, J. Alcami, E. Mira, and C. Martinez-A. 2000. Membrane raft microdomains mediate lateral assemblies required for HIV-1 infection. *EMBO Rep.* 1:190–196.

Mitchell, D.A., A.J. Fadden, and K. Drickamer. 2001. A novel mechanism of carbohydrate recognition by the C-type lectins DC-SIGN and DC-SIGNR. Subunit organization and binding to multivalent ligands. *J. Biol. Chem.* 276: 28939–28945.

Panyi, G., M. Bagdany, A. Bodnar, G. Vamosi, G. Szentesi, A. Jenei, L. Matyus, S. Varga, T.A. Waldmann, R. Gaspar, and S. Damjanovich. 2003. Colocalization and nonrandom distribution of Kv1.3 potassium channels and CD3 molecules in the plasma membrane of human T lymphocytes. *Proc. Natl. Acad. Sci. USA.* 100:2592–2597.

Percherancier, Y., B. Lagane, T. Planchenault, I. Staropoli, R. Altmeyer, J.L. Virelizer, F. Arenzana-Seisdedos, D.C. Hoessli, and F. Bachelerie. 2003. HIV-1 entry into T-cells is not dependent on CD4 and CCR5 localization to sphingolipid-enriched, detergent-resistant, raft Membrane Domains. *J. Biol. Chem.* 278:3153–3161.

Pöhlmann, S., J. Zhang, F. Baribaud, Z. Chen, G.J. Leslie, G. Lin, A. Granelli-Piperno, R.W. Doms, C.M. Rice, and J.A. McKeating. 2003. Hepatitis C virus glycoproteins interact with DC-SIGN and DC-SIGNR. *J. Virol.* 77: 4070–4080.

Rosenberger, C.M., J.H. Brumell, and B.B. Finlay. 2000. Microbial pathogenesis: lipid rafts as pathogen portals. *Curr. Biol.* 10:R823–R825.

Schuck, S., M. Honsho, K. Ekroos, A. Shevchenko, and K. Simons. 2003. Resistance of cell membranes to different detergents. *Proc. Natl. Acad. Sci. USA.* 100:5795–5800.

Simons, K., and D. Toomre. 2000. Lipid rafts and signal transduction. *Nat. Rev. Mol. Cell Biol.* 1:31–39.

Simons, K., and R. Ehehalt. 2002. Cholesterol, lipid rafts, and disease. *J. Clin. Invest.* 110:597–603.

Soilleux, E.J., R. Barten, and J. Trowsdale. 2000. DC-SIGN; a related gene, DC-SIGNR; and CD23 form a cluster on 19p13. *J. Immunol.* 165:2937–2942.

Stahl, P.D., and R.A. Ezekowitz. 1998. The mannose receptor is a pattern recognition receptor involved in host defense. *Curr. Opin. Immunol.* 10:50–55.

Steinman, R.M. 1991. The dendritic cell system and its role in immunogenicity. *Annu. Rev. Immunol.* 9:271–296.

Tailleux, L., O. Schwartz, J.L. Herrmann, E. Pivert, M. Jackson, A. Amara, L. Legres, D. Dreher, L.P. Nicod, J.C. Gluckman, et al. 2003. DC-SIGN is the major *Mycobacterium* tuberculosis receptor on human dendritic cells. *J. Exp. Med.* 197:121–127.

Tassaneetrithep, B., T.H. Burgess, A. Granelli-Piperno, C. Trumpfheller, J. Finke, W. Sun, M.A. Eller, K. Pattanapanyasat, S. Sarasombath, D.L. Birx, et al. 2003. DC-SIGN (CD209) mediates Dengue virus infection of human dendritic cells. *J. Exp. Med.* 197:823–829.

Turville, S.G., P.U. Cameron, A. Handley, G. Lin, S. Pöhlmann, R.W. Doms, and A.L. Cunningham. 2002. Diversity of receptors binding HIV on dendritic cell subsets. *Nat. Immunol.* 3:975–983.

van Die, I., S.J. van Vliet, A.K. Nyame, R.D. Cummings, C.M. Bank, B. Appelmelk, T.B. Geijtenbeek, and Y. van Kooyk. 2003. The dendritic cell specific C-type lectin DC-SIGN is a receptor for *Schistosoma mansoni* egg antigens and recognizes the glycan antigen Lewis-x. *Glycobiology.* 13:471–478.

Vereb, G., J. Matko, G. Vamosi, S.M. Ibrahim, E. Magyar, S. Varga, J. Szollosi, A. Jenei, R. Jr. Gaspar, T.A. Waldmann, and S. Damjanovich. 2000. Cholesterol-dependent clustering of IL-2Ra and its colocalization with HLA and CD48 on T lymphoma cells suggest their functional association with lipid rafts. *Proc. Natl. Acad. Sci. USA.* 97:6013–6018.

Vestweber, D., and J.E. Blanks. 1999. Mechanisms that regulate the function of the selectins and their ligands. *Physiol. Rev.* 79:181–213.